Front. Mech. Eng. 2019, 14(3): 273–281
https://doi.org/10.1007/s11465-018-0495-9

REVIEW ARTICLE

Shuncong ZHONG

# Progress in terahertz nondestructive testing: A review



**Abstract** Terahertz (THz) waves, whose frequencies range between microwave and infrared, are part of the electromagnetic spectrum. A gap exists in THz literature because investigating THz waves is difficult due to the weak characteristics of the waves and the lack of suitable THz sources and detectors. Recently, THz nondestructive testing (NDT) technology has become an interesting topic. This review outlines several typical THz devices and systems and engineering applications of THz NDT techniques in composite materials, thermal barrier coatings, car paint films, marine protective coatings, and pharmaceutical tablet coatings. THz imaging has higher resolution but lower penetration than ultrasound imaging. This review presents the significance and advantages provided by the emerging THz NDT technique.

**Keywords** terahertz pulsed imaging (TPI), nondestructive testing (NDT), composite material, thermal barrier coating

## 1 Introduction

Terahertz (THz) nondestructive testing (NDT) technology provides capabilities for noncontact inspection, high precision, and good penetration for non-conducting materials, such as ceramics and plastics. This technology is a powerful tool for biomedical, communication, and national defense applications. THz NDT applications have been delayed for many years because of the inefficiency of THz emission and detection devices. This condition is the so-called "THz gap" in this period. However, this gap has been addressed by the fast development of semiconductors and ultrafast electronics, and THz NDT has been widely applied in many fields over the last two decades. THz emitters and detectors are the main components of THz systems. Two THz sources are generally used: Continuous-wave (CW) and pulsed THz radiations. For example, CW THz waves can be generated by photomixing in low-temperature-grown gallium arsenide (GaAs) [1,2], quantum cascade lasers [3], and free-electron lasers [4], and whist pulsed THz waves can be produced by generating an ultrafast photocurrent in semiconductors illuminated by a femtosecond (fs) laser pulse, which result in electric field carrier acceleration [5]. For THz detectors, low-temperature-grown GaAs is normally used as a photoconductive antenna (PCA) [6]. Electro-optic sampling of THz radiation [7] is also a common technique for time-domain THz detection.

The source spectrum of a CW THz system is relatively narrow; therefore, limited information can be obtained (e.g., sometimes, only the intensity information is recorded) [8]. Unlike a CW system, a broadband emission of up to several THz can be achieved by a pulsed system, in which the time-domain THz wave (including intensity and phase information) can be recorded. THz pulsed imaging (TPI) can be used to nondestructively determine the properties of materials over the millimeter and sub-millimeter spectral ranges (0.1–10 THz), including pharmaceutical tablet coatings [9–12], marine protective coatings [13], automotive paints [14], polymer coatings [15], art paintings [16], public security [17,18], and medical applications [19,20]. Furthermore, recent THz developments have extended the applications of the nondestructive evaluation of composite materials [21–23] and thermal barrier coatings (TBCs) [24–26].

In this review, typical THz devices and THz spectroscopy and imaging systems are described. Furthermore, THz NDT applications in composite materials, industrial paints (e.g., car paints), TBCs, marine protective coatings, and pharmaceutical tablet coatings are presented. The trends of THz NDT techniques are also discussed.

## 2 Terahertz devices and systems

THz systems have revolutionized over the past two decades [27]. In this period, THz pulsed spectroscopy

Received May 26, 2017; accepted September 28, 2017

Shuncong ZHONG (✉)
Laboratory of Optics, Terahertz and Non-Destructive Testing, School of Mechanical Engineering and Automation, Fuzhou University, Fuzhou 350116, China; School of Mechatronic Engineering and Automation, Shanghai University, Shanghai 200072, China
E-mail: zhongshuncong@hotmail.com

(TPS) and TPI systems have been developed and commercialized. Figure 1 demonstrates the experimental setup of a typical transmission TPS system [28]. THz is generated and detected using an ultrafast fs laser (e.g., Ti: Sapphire laser). A beam splitter is used to separate the laser light into probe and pump beams. THz pulses are generated by a typically biased PCA or THz emitter. THz pulses emitted from the PCA under the illustration of the fs laser are focused on the sample by using Mirror 1 (off-axis elliptic mirror). The transmitted THz pulses are subsequently focused using a second off-axis elliptic mirror (Mirror 2) on an unbiased PCA for detection.

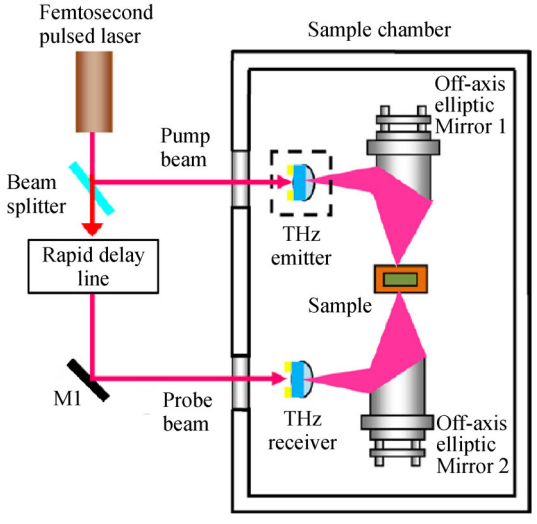


**Fig. 1** Experimental setup of typical transmission THz pulsed spectroscopy (TPS) system [28]

As shown in Fig. 1, the unbiased PCA is the important component of the TPS system. The structure of a typical PCA [29,30] is shown in Fig. 2. Typical gold bowtie-shaped antennas are fabricated on a low-temperature-grown GaAs semiconductor substrate. The antenna is biased with a direct-current voltage and illuminated with fs laser pulses. Photo-excited carriers at the photoconductive gap are excited and accelerated under the biased electric field. Subsequently, an ultrashort current pulse that produces THz radiation is generated. The transient current decays with a time constant, which is determined by the carrier lifetime in the semiconductor substrate. Normally, silicon (Si) lens is used to collect THz radiation [30], as shown in Fig. 1.

Although this THz emitter is widely used in THz spectroscopy and imaging systems, it has limited THz emission power, thereby limiting the important applications of THz NDT technology. Real-life applications require a novel THz antenna with less pump power than

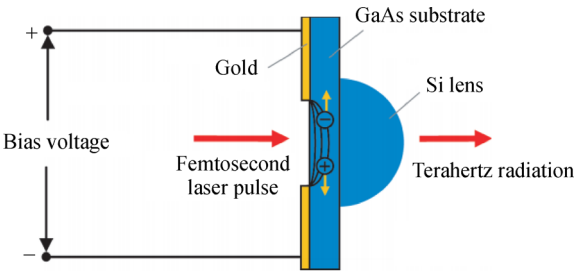


**Fig. 2** Typical biased THz emitter [30]

an fs laser pulse but can generate THz pulses with high-power output [30]. High THz wave power generally allows thick materials to be inspected due to improved signal-to-noise ratio. High-power THz devices can be manufactured using local field enhancement, which is induced by resonant plasmons, and static electric field enhancement. Currently, high-power THz radiation [31,32] is still a popular topic in high-power THz NDT applications.

TPI is capable of the three dimensional (3D) nondestructive inspection of materials. The core technology is essentially the same as that of TPS (Fig. 1) and TPI systems (Fig. 3). A TPI system has a six-axis robot system for *X*-*Y* movement and rotation of the material sample during the entire measurement. This arrangement ensures that the surface of the sample is always perpendicular to the THz beam and at the THz focus position [33].

As shown in Fig. 4 [11], the coating thickness of a coated structure can be achieved directly from the time delay between the interface and surface reflections. The coating thickness is calculated as the time delay divided by the refractive index (RI) of the coating material. Several other THz parameters (e.g., peak intensity and interface) can also be extracted simultaneously from the same THz time-domain waveform.

THz waveforms, which are recorded as a function of optical time delay, are collected at many points in the area of interest to map the surface of a sample during TPI measurement. Imaging an entire sample through point-by-point TPI measurement is time consuming. Therefore, high-speed THz imaging has become a research area of interest for real-time imaging applications. A spinning disk-based THz compressive sensing (CS) configuration was reported for high-speed image acquisition [34–36]. Furthermore, a single rotating random-binary-pattern mask was used to spatially modulate a collimated THz beam. After penetrating the sample, the THz waves could be measured using a single detector. Subsequently, THz images were reconstructed using the CS algorithm. The spinning disk could be rotated using an electric motor; thus, the compressed THz imaging system could work automatically and continuously. This system has significant potential for real-time THz imaging applications.

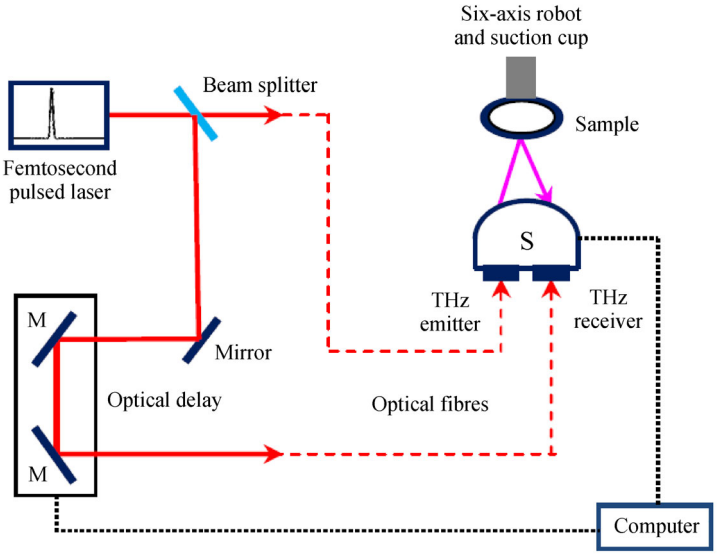


**Fig. 3** Terahertz pulsed imaging (TPI) system [33]

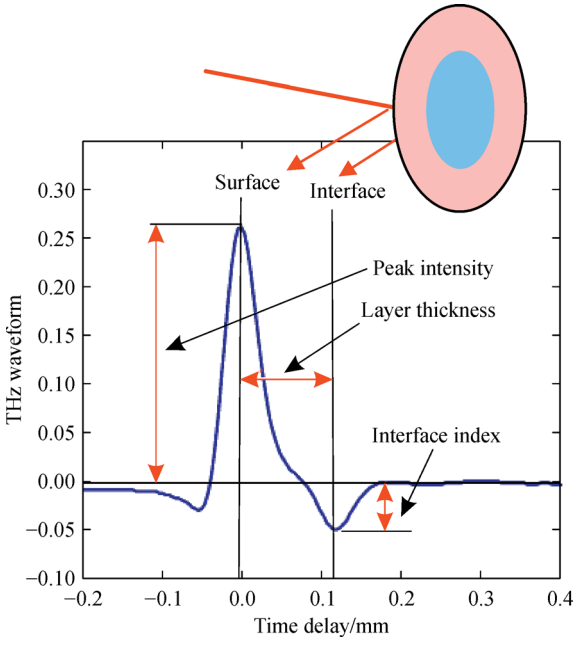


**Fig. 4** Typical THz waveform measured from single-layer-coated structure [11]

## 3 Terahertz nondestructive testing

### 3.1 Composite materials

Composite materials are important in various application fields, such as aerospace, wind energy, and civil engineering, because they have high mechanical strength and low weight [37]. However, defects, such as voids, inclusions, delamination, and cracks, are often produced in the manufacturing process of composite materials. In addition, defects are generated during the life cycle of composite material structures. To ensure the structural integrity of these structures, defects should be detected and localized. THz technology with high resolution and good penetration has recently become a promising NDT technique for defect detection in composite materials. THz pulsed waveforms are measured through TPI, as shown in Fig. 5(a) [38]. Fast Fourier transform can be used to obtain the time-domain THz wave, frequency amplitude (Fig. 5(b)), and the corresponding phase information, from which the internal information of the composite material can be achieved.

TPI is sensitive to fiber orientation detection. Figures 6(a) and 6(b) [39] show regular and irregular fiber orientations captured by C-scans. As an example of a defect occurring during the production phase of a composite laminate, an inclusion is presented in Figs. 6 (c) and 6(d) [39]. The detectability of this inhomogeneity depends on the difference between the RIs of the examined object and the inclusion material. The measurement results of delamination and the dangerous defect occurring during the application phase are shown in Figs. 6(e) and 6(f) [39]. This example demonstrates the NDT capability of TPI on composite materials with different defects.

Unlike ultrasound imaging, TPI is noncontact in nature and does not require the liquid to couple the ultrasonic wave from the transducer to examine composite materials. Figure 7 shows sample images of a fiber composite imaged by TPI and ultrasound imaging [40]. The fiber composite measures 165 mm × 20 mm (neck = 13 mm) × 4 mm and has buried voids of approximately 100 μm [40]. In Fig. 7, the buried void can be clearly detected by THz imaging. By contrast, ultrasonic imaging cannot clearly provide the damage information. The imaging resolution of THz is

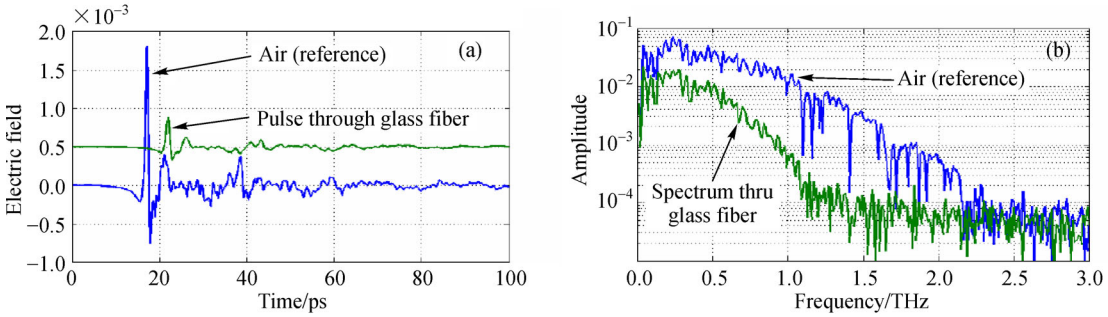


**Fig. 5** Measured THz pulsed waveforms. (a) Time-domain waveform [38]; (b) frequency amplitude spectra

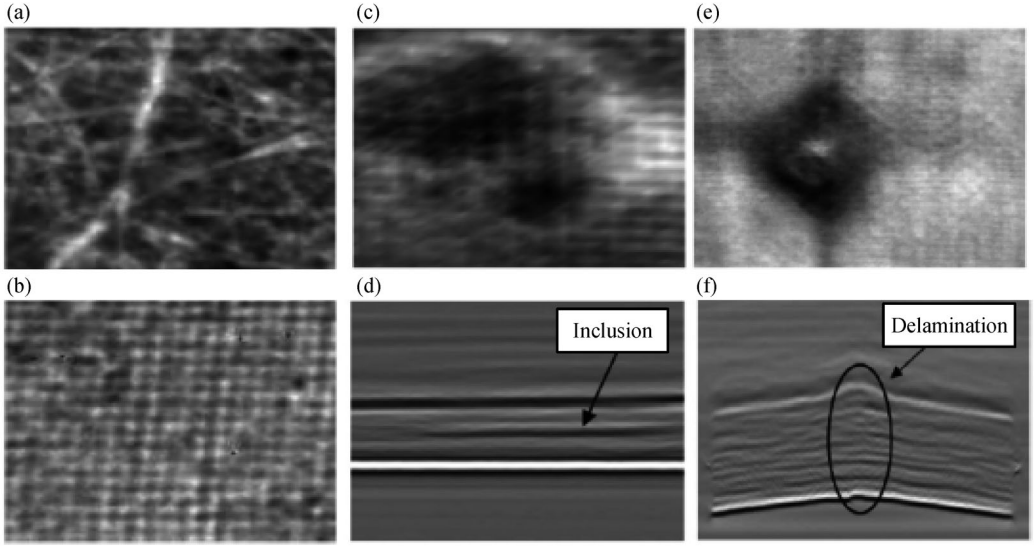


**Fig. 6** THz NDT measurements of glass fiber composite material [39]. (a) Irregular fiber orientation (C-scan); (b) regular fiber orientation (C-scan); (c) C-scan of inclusion; (d) B-scan of inclusion; (e) C-scan of delamination; (f) B-scan of delamination

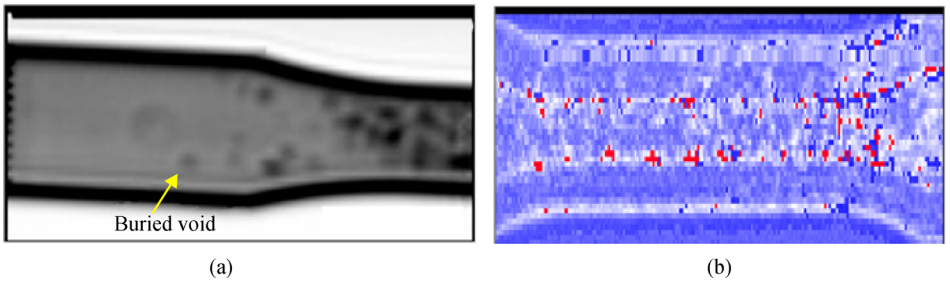


**Fig. 7** Fiber composite imaged by (a) THz and (b) ultrasound [40]

higher than that of ultrasound imaging in terms of clear buried void detection on fiber composites. Normally, the resolution of ultrasonic imaging is approximately 100 μm but still depends on ultrasonic frequency, and the resolution of TPI is approximately 20–30 μm. Meanwhile, the penetration depth of THz waves is less than that of ultrasonic waves, which can propagate through metal and non-metal materials; THz waves can be used only for non-conducting materials.

### 3.2 Thermal barrier coatings

A TBC is an advanced material system that is applied on high-temperature metallic surfaces, such as gas turbines and aero engines. Normally, a TBC system includes a ceramic topcoat and a metallic bondcoat [27] on metal substrates (e.g., NiCrAlY or NiCoCrAlY alloy), as shown in Fig. 8. The RIs of air, topcoat, and bondcoat are $n_0$, $n_1$, and $n_2$, respectively, and follow this relationship:

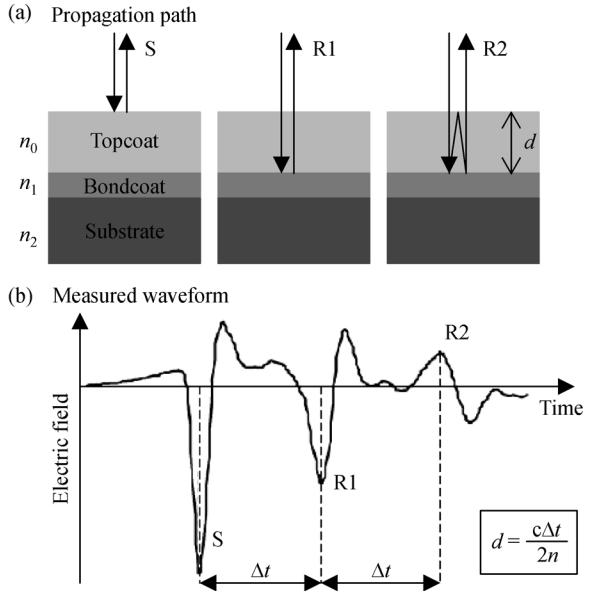


**Fig. 8** Thickness measurement of TBC topcoat using THz waves [41]. (a) Schematic diagram of the terahertz propagation path; (b) waveform of the terahertz wave measured

$n_0 < n_1 < n_2$. During field service of a TBC system, several damages or defects are initialized and propagated, such as delamination, coat thinning, and gradual formation of a thermally grown oxide (TGO) thin film. Several reflections appear on the topcoat surface (S) and interfaces (such as R1 and R2) when a THz wave pulse is incident on TBC. The reflection coefficients of S, R1, and R2 can be calculated as $(n_0-n_1)/(n_0+n_1)$, $(n_1-n_2)/(n_1+n_2)$, and $(n_1-n_0)/(n_1+n_0)$, respectively. The reflection coefficients of S, R1, and R2 are negative, negative, and positive, respectively, because $n_0 < n_1 < n_2$. These findings explain why the waveforms from the paths of S and R1 in Fig. 8 are valleys, and the result from R2 is a peak wave. The corresponding time-domain THz waveform, from which the coating thickness of the topcoat can be achieved, is shown in Fig. 8 [41].

The topcoat thickness measured by THz agrees with the measurement results by microscope observation, and the difference is within the range of measurement error [42,43]. This finding demonstrates the high potential application of THz waves in NDT or structural health monitoring of TBC systems. By contrast, the typical thickness of a TGO layer is normally approximately a few micrometers (e.g., 10 μm) before TBC peeling. This condition indicates that TGO thickness is generally smaller than the pulse width of the THz waveform; hence, a TGO layer cannot be sufficiently detected by THz waves. Therefore, the use of high-resolution THz techniques for TGO layer detection remains an issue.

Chen et al. [44] conducted the pioneering work in TGO measurement by THz. They employed time-domain THz reflectometry for the health monitoring of a TGO layer.

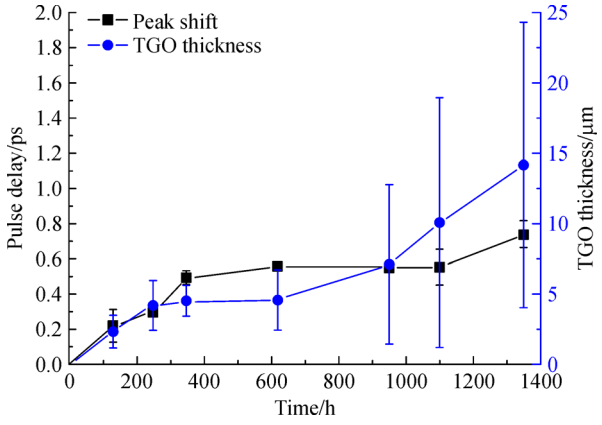


**Fig. 9** Comparison of averaged TGO thickness (SEM method) and delay time (THz method) [44]

Figure 9 demonstrates that the THz pulse delay time increases with a 348 h thermal exposure. The TGO layer is also measured by scanning electron microscope (SEM), which reveals increases in TGO thickness from 0 to 5 μm with a 348 h thermal exposure and to 9 μm with a 1300 h thermal exposure. The changes in TGO thickness with the increase in thermal exposure time can be distinguished by the increased pulse delays of the THz pulses reflected from the TBC system (multilayered structure). This finding can be used for TBC health monitoring [44].

### 3.3 Car paints and marine coatings

Car paints have several important functions, such as giving distinct colors to cars and providing protection from corrosion, ultraviolet radiation, and scratches. Therefore, painting is an important step during automotive manufacturing. Several traditional methods are used to characterize the thickness of paint layers, such as ultrasound testing (UT), X-ray microcomputed tomography (CT), and eddy current (EC). The UT and EC methods are contact measurement techniques; that is, the measurement sensors or probes need to be in contact with the painted car surface. Meanwhile, the safety of using X-ray should be considered in using the CT technique in real engineering applications. THz time-domain spectroscopy has been reported as a noncontact NDT technique for thin car paint layers. Yasui et al. [45] and Izutanni et al. [46] demonstrated the use of a THz paint meter for the noncontact measurement of the thickness of thin film paint. Furthermore, Yasuda et al. [47] proposed a fitting method to enhance the sensitivity of minimum thickness measurement. Su et al. [48,49] demonstrated excellent THz NDT performance in evaluating the thickness of car paint films. Figure 10 shows the B-scan map and time-domain reflection waveform of a single pixel [48]. The reflection peaks at all interfaces between different thin film paints can be identified effectively.

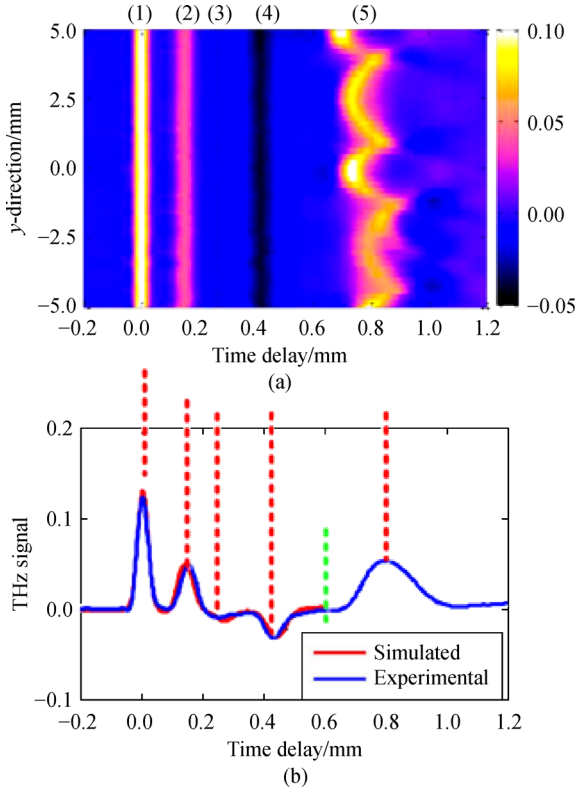


**Fig. 10** TPI reflected waveform of multilayered car paint on carbon fiber substrate [48]. (a) B-scan map measured along the *y*-direction. (b) time-domain reflection waveform of a single pixel

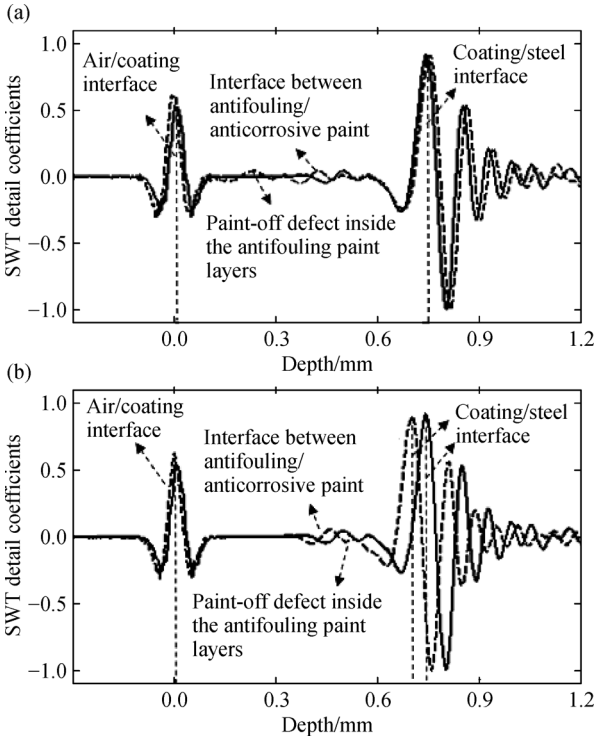


**Fig. 11** Comparisons of SWT detail coefficients for intact and defected marine protective coatings [52]. A defect with radius of 12 mm and thickness of 0.18 mm was embedded inside (a) the three antifouling paint layers and (b) the anticorrosive paint layers

The thickness of the multilayered car paint sample, which consists of four layers, is measured by TPI and traditional methods, namely, UT, EC, and CT. Comparison results show that THz has good consistency with the other methods; therefore, THz time-domain systems are ideal for thickness measurements and analysis of layered structures [48]. In these NDT applications, time-domain THz waveforms are used to image the inner structures of multilayered paint films similarly as ultrasound imaging techniques do. In comparison with the traditional techniques UT, CT, and EC, the TPI technique is more advantageous because it is noncontact in nature. In addition, TPI is able to spatially obtain the thickness uniformity distribution information from the 2D THz images.

Protective coating is usually applied on the surfaces of marine or offshore structures for corrosion protection. The usage of THz waves for marine coating detection has attracted significant attention. Cook et al. [50,51] discussed the applicability of THz NDT for marine protective coatings and conducted a laboratory experiment to measure the dry film thickness of organic coatings. Recently, Tu et al. [52] demonstrated the TPI NDT of marine protective coatings using the finite-difference time-domain method combined with the stationary wavelet transform (SWT) approach. As shown in Fig. 11 [52], defects underneath marine protective coatings can be detected by TPI technology. The results demonstrate that TPI technology can be an excellent means of the health monitoring of protective coatings.

### 3.4 Pharmaceutical coatings

Pharmaceutical tablet coating is the preferred means for the release control of active pharmaceutical ingredients (API). For example, sustained-release coating is used to achieve an optimized release profile and a desirable API absorption rate [10]. According to the pioneering work on nondestructive analysis of tablet coatings by Fitzgerald et al. [53], TPI is a powerful tool for the nondestructive, noncontact determination of the tablet coating thickness of single-film- and multifilm-coated tablets. Figure 12 shows images of the 3D coating thickness of a coated biconvex tablet and their uniformity [55]. The tablet is coated with a sustained-release film coating on the tablet core. The tablet core comprises lactose monohydrate with vinylpyrrolidone-vinyl acetate copolymer, and the ingredients of the tablet coating are Kollidon VA-64®, polyvinyl acetate, and polyvinyl alcohol-polyethylene glycol graft copolymer [55]. The color bars in Fig. 12 show the coating thickness (varying from 70 to 180 μm) of two sides and the center band of the coated biconvex tablet and indicate that the

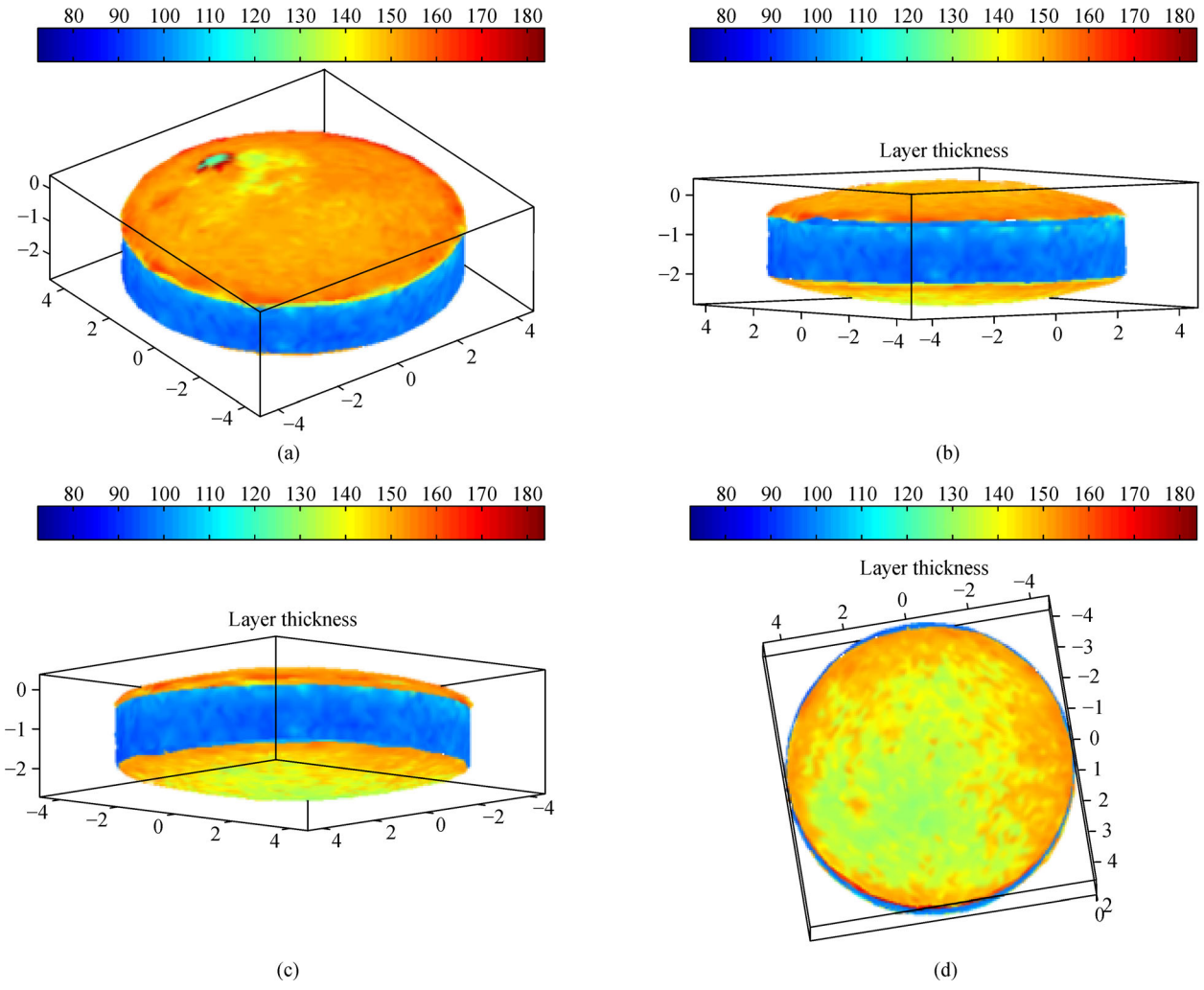


**Fig. 12** 3D coating thickness images on two sides and center band of coated biconvex tablet [55]. (a) Top side; (b) center band (front); (c) center band (back); (d) bottom side

thickness of the two sides of the tablet is larger than that of the tablet center band.

The capability of THz radiation to penetrate a sample and provide information about its inner structure makes TPI an excellent tool for identifying inner defects and buried structures [55–57]. May et al. [58] applied TPI in the pharmaceutical industry for the in-line real-time measurement of the coating thickness of randomly moving tablets coated with a production-scale pan coater. The direct TPI-based coating thickness analysis method has a significant impact on understanding the coating process.

## 4 Conclusions

THz NDT has attracted significant attention in recent years. Many countries are devoted to promoting THz NDT technology. Certain studies have demonstrated the significance of THz NDT technology in various applications. The THz NDT technique has superiority in inspecting the hidden defects of materials through noncontact means because THz radiation is transparent in most nonconducting materials. For example, the THz NDT of composite materials, TBCs, car paints, marine protective coatings, and pharmaceutical tablet coatings are discussed in this review. THz NDT is a powerful technique that allows nondestructive high-resolution cross-sectional imaging. In comparison with traditional NDT methods, such as UT, EC, and CT, THz NDT provides a wider range of advantages, including noncontact nature and high sensitivity and resolution.

However, the cost of TPI systems is relatively high and therefore limits their engineering applications. The current spatial resolution of THz systems is approximately 20–30 μm, which cannot meet the requirement of the structural health monitoring of the small TGO thickness of TBC systems. Furthermore, high-power THz radiation remains a major issue for THz NDT applications, which occasionally

require high-penetration inspections with high signal-to-noise ratio.

Therefore, THz systems should be made fast and affordable to extend THz NDT applications in industries, which requires new approaches to obtaining many details of THz system architectures. In addition, the spectral range of current instruments should be extended to potentially provide high spatial resolution for the effective NDT of materials, especially for small initial defects or thin films (e.g., TGO). Meanwhile, advanced signal processing methods for feature extraction with weak defect information is an option for THz NDT. The penetration depth of THz waves should also be investigated. High-power THz radiation, which achieves thick materials for inspection, is desirable in engineering applications.

**Acknowledgements** We would like to express our appreciation to the National Natural Science Foundation of China (Grant No. 51675103), Fujian Provincial Excellent Young Scientist Fund (Grant No. 2014J07007), Shanghai Natural Science Fund (Grant No. 18ZR1414200), and Research Project of State Key Laboratory of Mechanical System and Vibration (Grant No. MSV201807).

## References

1. Brown E, McIntosh K, Nichols K, et al. Photomixing up to 3.8 THz in low-temperature-grown GaAs. Applied Physics Letters, 1995, 66 (3): 285–287
2. Gu P, Tani M, Hyodo M, et al. Generation of cw-terahertz radiation using a two-longitudinal-mode laser diode. Japanese Journal of Applied Physics, 1998, 37, Part 2(8B): L976–L978
3. Smet J, Fonstad C, Hu Q. Intrawell and interwell intersubband transitions in multiple quantum wells for far-infrared sources. Journal of Applied Physics, 1996, 79(12): 9305–9320
4. Jeong Y, Lee B, Kim S, et al. First lasing of the KAERI compact far-infrared free-electron laser driven by a magnetron-based microtron. Nuclear Instruments & Methods in Physics Research. Section A, Accelerators, Spectrometers, Detectors and Associated Equipment, 2001, 475(1–3): 47–50
5. Tonouchi M. Cutting-edge terahertz technology. Nature Photonics, 2007, 1(2): 97–105
6. Shen Y, Upadhya P, Linfield E, et al. Terahertz generation from coherent optical phonons in a biased GaAs photoconductive emitter. Physical Review B: Condensed Matter and Materials Physics, 2004, 69(23): 235325
7. Tani M, Horita K, Kinoshita T, et al. Efficient electro-optic sampling detection of terahertz radiation via Cherenkov phase matching. Optics Express, 2011, 19(21): 19901–19906
8. Yu C, Fan S, Sun Y, et al. The potential of terahertz imaging for cancer diagnosis: A review of investigations to date. Quantitative Imaging in Medicine and Surgery, 2012, 2(1): 33–45
9. Ho L, Müller R, Gordon K C, et al. Terahertz pulsed imaging as an analytical tool for sustained-release tablet film coating. European Journal of Pharmaceutics and Biopharmaceutics, 2009, 71(1): 117–123
10. Zhong S, Shen Y, Ho L, et al. Non-destructive quantification of pharmaceutical tablet coatings using terahertz pulsed imaging and optical coherence tomography. Optics and Lasers in Engineering, 2011, 49(3): 361–365
11. Shen Y. Terahertz pulsed spectroscopy and imaging for pharmaceutical applications: A review. International Journal of Pharmaceutics, 2011, 417(1–2): 48–60
12. Lin H, Dong Y, Markl D, et al. Measurement of the intertablet coating uniformity of a pharmaceutical pan coating process with combined terahertz and optical coherence tomography in-line. Journal of Pharmaceutical Sciences, 2017, 106(4): 1075–1084
13. Tu W, Zhong S, Shen Y, et al. Nondestructive testing of marine protective coatings using terahertz waves with stationary wavelet transform. Ocean Engineering, 2016, 111: 582–592
14. Su K, Shen Y, Zeitler J A. Terahertz sensor for non-contact thickness and quality measurement of automobile paints of varying complexity. IEEE Transactions on Terahertz Science and Technology, 2014, 4(4): 432–439
15. Dong J, Locquet A, Citrin D S. Terahertz quantitative nondestructive evaluation of failure modes in polymer-coated steel. IEEE Journal of Selected Topics in Quantum Electronics, 2017, 23(4): 8400207
16. Dong J, Bianca Jackson J, Melis M, et al. Terahertz frequency-wavelet domain deconvolution for stratigraphic and subsurface investigation of art painting. Optics Express, 2016, 24(23): 26972–26985
17. Shen Y, Lo T, Taday P F, et al. Detection and identification of explosives using terahertz pulsed spectroscopic imaging. Applied Physics Letters, 2005, 86(24): 241116
18. Federici J F, Schulkin B, Huang F, et al. THz imaging and sensing for security applications—Explosives, weapons and drugs. Semiconductor Science and Technology, 2005, 20(7): S266–S280
19. Woodward R M, Wallace V P, Arnone D D, et al. Terahertz pulsed imaging of skin cancer in the time and frequency domain. Journal of Biological Physics, 2003, 29(2–3): 257–259
20. Crawley D, Longbottom C, Wallace V P, et al. Three-dimensional terahertz pulse imaging of dental tissue. Journal of Biomedical Optics, 2003, 8(2): 303–307
21. Naito K, Kagawa Y, Utsuno S, et al. Dielectric properties of eight-harness-stain fabric glass fiber reinforced polyimide matrix composite in the THz frequency range. NDT & E International, 2009, 42(5): 441–445
22. Stoik C, Bohn M, Blackshire J. Nondestructive evaluation of aircraft composites using reflective terahertz time domain spectroscopy. NDT & E International, 2010, 43(2): 106–115
23. Lopato P. Double-sided terahertz imaging of multilayered glass fiber-reinforced polymer. Applied Sciences, 2017, 7(7): 661–674
24. Watanabe M, Kuroda S, Yamawaki H, et al. Terahertz dielectric properties of plasma-sprayed thermal-barrier coatings. Surface and Coatings Technology, 2011, 205(19): 4620–4626
25. Fukuchi T, Fuse N, Okada M, et al. Topcoat thickness measurement of thermal barrier coating of gas turbine blade using terahertz wave. Electrical Engineering in Japan, 2014, 189(1): 1–8
26. Roth D J, Cosgriff L M, Harder B, et al. Self-calibrating terahertz technique for measuring coating thickness. Materials Evaluation, 2015, 73(9): 1205–1213
27. Ferguson B, Zhang X C. Materials for terahertz science and

technology. Nature Materials, 2002, 1(1): 26–33
28. Strachan C J, Rades T, Newnham D A, et al. Using terahertz pulsed spectroscopy to study crystallinity of pharmaceutical materials. Chemical Physics Letters, 2004, 390(1–3): 20–24
29. Cheville R A, Grischkowsky D. Far-infrared terahertz time-domain spectroscopy of flames. Optics Letters, 1995, 20(15): 1646–1648
30. Zhong S, Shen Y, Shen H, et al. FDTD study of a novel terahertz emitter with electrical field enhancement using surface plasmon resonance. PIERS Online, 2010, 6(2): 153–156
31. Yoneda H, Tokuyama K, Ueda K, et al. High-power terahertz radiation emitter with a diamond photoconductive switch array. Applied Optics, 2001, 40(36): 6733–6736
32. Ropagnol X, Morandotti R, Ozaki T, et al. Toward high-power terahertz emitters using large aperture ZnSe photoconductive antennas. IEEE Photonics Journal, 2011, 3(2): 174–186
33. Zhong S, Shen Y, Evans M, et al. Quantification of thin-film coating thickness of pharmaceutical tablets using wavelet analysis of terahertz pulsed imaging data. In: Proceedings of 34th International Conference on Infrared, Millimeter, and Terahertz Waves, IRMMW-THz. Busan: IEEE, 2009
34. Shen H, Gan L, Newman N, et al. Spinning disk for compressive imaging. Optics Letters, 2012, 37(1): 46–48
35. Shen H, Newman N, Gan L, et al. Compressed terahertz imaging system using a spin disk. In: Proceedings of IEEE International Conference on Infrared, Millimetre, and Terahertz Waves (IRMMW-THz 2010). Rome: IEEE, 2010, 3–4
36. Liu L, Zhang Z, Gan L, et al. Terahertz Imaging with compressed sensing. In: Proceedings of IEEE 9th UK-Europe-China Workshop on Millimetre Waves and Terahertz Technologies (UCMMT 2016). Qingdao: IEEE, 2016, 50–53
37. Amenabar I, Lopez F, Mendikute A. In introductory review to THz non-destructive testing of composite material. Journal of Infrared, Millimeter, and Terahertz Waves, 2013, 34(2): 152–169
38. Stoik C D, Bohn M J, Blackshire J L. Nondestructive evaluation of aircraft composites using transmissive terahertz time domain spectroscopy. Optics Express, 2008, 16(21): 17039
39. Chady T, Przemyslaw P. Testing of glass-fiber reinforced composite materials using terahertz technique. International Journal of Applied Electromagnetics and Mechanics, 2010, 33(3–4): 1599–1605
40. Anbarasu A. Characterization of defects in fiber composites using terahertz imaging. Thesis for the Master's Degree. Atlanta: Georgia Institute of Technology, 2008
41. Fukuchi T, Ozeki T, Okada M, et al. Nondestructive inspection of thermal barrier coating of gas turbine high temperature components. IEEJ Transactions on Electrical and Electronic Engineering, 2016, 11(4): 391–400
42. Fukuchi T, Fuse N, Okada M, et al. Topcoat thickness measurement of thermal barrier coating of gas turbine blade using terahertz wave. Electrical Engineering in Japan, 2014, 189(1): 1–8
43. Fukuchi T, Fuse N, Okada M, et al. Measurement of refractive index and thickness of topcoat of thermal barrier coating by reflection measurement of terahertz waves. Electronics and Communications in Japan, 2013, 96(12): 37–45
44. Chen C, Lee D, Pollock T, et al. Pulsed-terahertz reflectometry for health monitoring of ceramic thermal barrier coatings. Optics Express, 2010, 18(4): 3477–3486
45. Yasui T, Yasuda T, Sawanaka K, et al. Terahertz paintmeter for noncontact monitoring of thickness and drying progress in paint film. Applied Optics, 2005, 44(32): 6849–6856
46. Izutani Y, Akagi M, Kitagishi K. Measurements of paint thickness of automobiles by using THz time-domain spectroscopy. In: Proceedings of 37th International Conference on Infrared, Millimeter, and Terahertz Waves. Wollongong: IEEE, 2012
47. Yasuda T, Iwata T, Araki T, et al. Improvement of minimum paint film thickness for THz paint meters by multiple-regression analysis. Applied Optics, 2007, 46(30): 7518–7526
48. Su K, Shen Y, Zeitler J A. Terahertz sensor for non-contact thickness and quality measurement of automobile paints of varying complexity. IEEE Transactions on Terahertz Science and Technology, 2014, 4(4): 432–439
49. Su K, May R K, Gregory I S, et al. Terahertz sensor for non-contact thickness measurement of car paints. In: Proceedings of 38th International Conference on Infrared, Millimeter, and Terahertz Waves (IRMMW-THz). Mainz: IEEE, 2013
50. Cook D J, Sharpe S J, Lee S, et al. Terahertz time domain measurements of marine paint thickness. Optical Terahertz Science and Technology, 2007, TuB5
51. Cook D J, Lee S, Sharpe S J, et al. Accuracy and linearity of time-domain THz paint thickness measurements. SPIE Proceedings, Terahertz Technology and Applications, 2008, 6893: 68930H
52. Tu W, Zhong S, Shen Y, et al. Nondestructive testing of marine protective coatings using terahertz waves with stationary wavelet transform. Ocean Engineering, 2016, 111: 582–592
53. Fitzgerald A J, Cole B E, Taday P F. Nondestructive analysis of tablet coating thicknesses using terahertz pulsed imaging. Journal of Pharmaceutical Sciences, 2005, 94(1): 177–183
54. Ho L, Müller R, Römer M, et al. Analysis of sustained-release tablet film coats using terahertz pulsed imaging. Journal of Controlled Release, 2007, 119(3): 253–261
55. Zeitler J A, Shen Y, Baker C, et al. Analysis of coating structures and interfaces in solid oral dosage forms by three dimensional terahertz pulsed imaging. Journal of Pharmaceutical Sciences, 2007, 96(2): 330–340
56. Wallace V P, Taday P F, Fitzgerald A J, et al. Terahertz pulsed imaging and spectroscopy for biomedical and pharmaceutical applications. Faraday Discussions, 2004, 126: 255–263
57. Ho L, Cuppok Y, Muschert S, et al. Effects of film coating thickness and drug layer uniformity on in vitro drug release from sustained-release coated pellets: A case study using terahertz pulsed imaging. International Journal of Pharmaceutics, 2009, 382(1–2): 151–159
58. May R K, Evans M J, Zhong S, et al. Terahertz in-line sensor for direct coating thickness measurement of individual tablets during film coating in real-time. Journal of Pharmaceutical Sciences, 2011, 100(4): 1535–1544